

S. Saarelma, M. Beurskens, C. Challis, L. Frassinetti, C. Giroud,  
M. Groth, A. Järvinen, M. Leyland, C. Maggi, J. Simpson, JET  
Contributors

# The effects of impurities and core pressure on pedestal stability in Joint European Torus (JET)

Enquiries about copyright and reproduction should in the first instance be addressed to the Culham Publications Officer, Culham Centre for Fusion Energy (CCFE), K1/083, Culham Science Centre, Abingdon, Oxfordshire, OX14 3DB, UK. The United Kingdom Atomic Energy Authority is the copyright holder.

# The effects of impurities and core pressure on pedestal stability in Joint European Torus (JET)

S. Saarelma<sup>1</sup>, M. Beurskens<sup>1</sup>, C. Challis<sup>1</sup>, L. Frassinetti<sup>2</sup>, C. Giroud<sup>1</sup>,  
M. Groth<sup>3</sup>, A. Järvinen<sup>3</sup>, M. Leyland<sup>4</sup>, C. Maggi<sup>1</sup>, J. Simpson<sup>1</sup>, JET  
Contributors

<sup>1</sup>*Culham Centre for Fusion Energy, Culham Science Centre, Abingdon, OX14 3DB, UK*

<sup>2</sup>*Division of Fusion Plasma Physics, School of Electrical Engineering, Royal Institute of  
Technology, Stockholm, Sweden*

<sup>3</sup>*Aalto University, Otakaari 4, 02150 Espoo, Finland*

<sup>4</sup>*York Plasma Institute, Department of Physics, University of York, Heslington, York,  
YO10 5DD, UK*



# The effects of impurities and core pressure on pedestal stability in Joint European Torus (JET)

S. Saarelma<sup>1</sup>, M. Beurskens<sup>1</sup>, C. Challis<sup>1</sup>, L. Frassinetti<sup>2</sup>, C. Giroud<sup>1</sup>, M. Groth<sup>3</sup>, A. Järvinen<sup>3</sup>, M. Leyland<sup>4</sup>, C. Maggi<sup>1</sup>, J. Simpson<sup>1</sup>, JET Contributors\*

EUROfusion Consortium JET Culham Science Centre, Abingdon, OX14 3DB, UK

<sup>1</sup>Culham Centre for Fusion Energy, Culham Science Centre, Abingdon, OX14 3DB, UK

<sup>2</sup>Division of Fusion Plasma Physics, School of Electrical Engineering, Royal Institute of Technology, Stockholm, Sweden

<sup>3</sup>Aalto University, Otakaari 4, 02150 Espoo, Finland

<sup>4</sup>York Plasma Institute, Department of Physics, University of York, Heslington, York, YO10 5DD, UK.

[samuli.saarelma@ccfe.ac.uk](mailto:samuli.saarelma@ccfe.ac.uk)

## Abstract

The H-mode pedestal plays an important role in determining global confinement in tokamaks. In high triangularity H-mode experiments in Joint European Torus with the ITER-like wall (JET-ILW), significantly higher pedestal temperature and global confinement has been achieved with nitrogen seeding. The experimental increase of pedestal height is consistent with the stability calculations which show that edge localised impurity concentration can increase the electron pressure pedestal at the point of marginal stability. Numerically found stability improvement mechanism from impurity seeding is a combination of moving the pedestal inwards and increasing the ion dilution.

Significantly better confinement and pedestal height have been observed in JET-ILW plasmas when the core pressure is increased. The enhanced pedestal height can be linked to an improvement in edge stability arising from an increase in the Shafranov-shift, higher edge current and pedestal widening in flux space.

\* See the Appendix of F. Romanelli et al., Proceedings of the 25th IAEA Fusion Energy Conference 2014, St Petersburg, Russia

## I. INTRODUCTION

The global plasma confinement in a tokamak operating in high confinement or H-mode is largely determined by the edge pedestal pressure due to core turbulence restricting the temperature gradient near the marginal stability limit [1]. The transport simulations using the TGLF show that the ITER fusion power scales like  $T_{ped}^2$  [2], where  $T_{ped}$  is the temperature at the top of the pedestal. The pedestal of Type I ELMy H-mode (the typical operation regime of current tokamaks and the baseline operation for ITER) has been shown to be limited by ideal MHD peeling-ballooning modes in JET [3], DIII-D [4], JT-60U [5] and ASDEX Upgrade [6]. Therefore, if the edge peeling-ballooning stability can be improved, higher pedestals and, consequently, better global plasma performance can be achieved. The shaping of plasma, especially increasing triangularity, has been shown experimentally and numerically to lead to higher pedestals [4]. This paper investigates two other possible mechanisms to increase the pedestal height to improve the performance: increasing core pressure and seeding of low-Z impurities.

## II. ANALYSIS METHOD

In this paper we analyse the pedestal stability of plasma equilibria. First we recreate the investigated equilibrium using the pedestal temperature and density profiles measured using the Thomson scattering systems [7,8,9]. The profiles are fitted with the modified tanh-function described in [10]. Since the standard equilibrium reconstruction is usually not accurate enough to give the separatrix location in relation to the profiles, we have to radially shift the measured profiles to be consistent with the power balance at the separatrix. In this paper we use a simple two-point model [11] to determine the separatrix electron temperature  $T_{e,sep}$  when there are no significant factors within an investigated scan to create differences between plasmas and more complete multi-fluid modelling using the EDGE2D-EIRENE code [12,13,14] when we assume that  $T_{e,sep}$  is strongly affected by changes in edge radiation. Since the density and temperature profiles are measured by the same diagnostic both are shifted by the same amount.

We assume that the current profile is composed of bootstrap and fully diffused Ohmic currents that are calculated self-consistently using the profiles and adjusting the Ohmic current amplitude so that the total current agrees with the experimental value. The bootstrap current is calculated using formulas in [15]. To find the stability boundaries we either perturb the normalised pedestal pressure gradient ( $\alpha$ ) and current density ( $j$ ) from the values of the experimental equilibrium to produce a  $j$ - $\alpha$  diagram showing the stability boundaries in relation to the investigated equilibrium or we vary the temperature pedestal height and calculate the current profile self-consistently to find the marginally stable temperature pedestal height. Whilst the former method gives us a general picture of the stability around the investigated plasma, it is not always very good for determining the distance from the marginal stability. On the other hand, the self-consistent method provides us a scalar value for the marginal stability, which can then be compared with the experimental pedestal height or other stability analysis results. In the stability calculations we use the ideal MHD stability code ELITE [16].

### III. POWER SCAN

To study the connection between the core pressure and the pedestal stability a power scan JET experiment at  $I_p=1.4$  MA and  $B_t=1.7$ T using neutral beam injection (NBI) only was conducted at low ( $\delta_u=0.2$ ) and high ( $\delta_u=0.4$ ) triangularity. The NBI heating power was varied between 4 and 15 MW. The gas injection rate was kept as low as possible while still ensuring high enough ELM frequency to avoid high tungsten influx and radiation. The resulting range of  $\beta_N$  was 1.5 to 3. More detailed description of the experiment is given in [17]. In the equilibrium reconstruction we used the density and temperature profiles that were in the last 30% of the ELM cycle. The change of the  $j$ - $\alpha$  stability diagram as  $\beta_N$  is increased is shown in Figure 1. For both low (1.5) and high  $\beta_N$  (3.0), the experimental equilibria are close to their respective stability boundaries. In the self-consistent analysis (vary the pedestal height from the experimental value to find the marginally stable pedestal height), we find that all the plasmas in the power scan are within measurement error from their

stability limit. At low power, there is no difference between low and high triangularity plasmas, but as the power is increased the high triangularity plasmas see larger increase both in measured and modelled pedestal height. The increase in marginally stable  $\alpha$  between the low and high  $\beta_N$  case is only about 50% (Fig. 2), while the pedestal height more than doubles. This is explained by the pedestal widening with increasing  $\beta_N$  allowing the pedestal height to increase without a corresponding increase in the gradient. The pedestals widen only in flux space. In real space (at the outboard midplane) the width does not increase, so the widening in flux space can be associated with the increasing Shafranov-shift that pushes the flux surfaces closer together on the outboard side. The self-consistent marginally stable pedestal height is also increased by decreasing pedestal collisionality that leads to higher bootstrap current. Higher edge current allows access to the “nose” of stability diagram and so achieves high values of  $\alpha$  without triggering the limiting peeling-ballooning modes. In Fig. 1., the self-consistent path of the  $\beta_N=3.0$  case crosses the stability boundary at the maximum value of  $\alpha$  allowed by the stability boundary, while the  $\beta_N=1.4$  becomes limited at  $\alpha=3.8$  even though the maximum  $\alpha$  allowed by the stability boundary at higher current density would be 4.1.

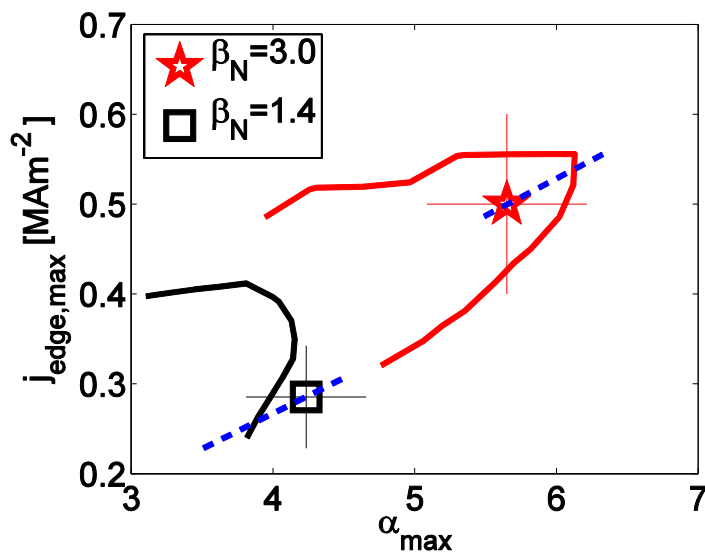


Figure 1. Stability boundaries and operational points of the lowest and the highest  $\beta_n$  values of the high  $\delta$  power scan. The dashed lines show the self-consistent path with varying  $T_{ped}$ .

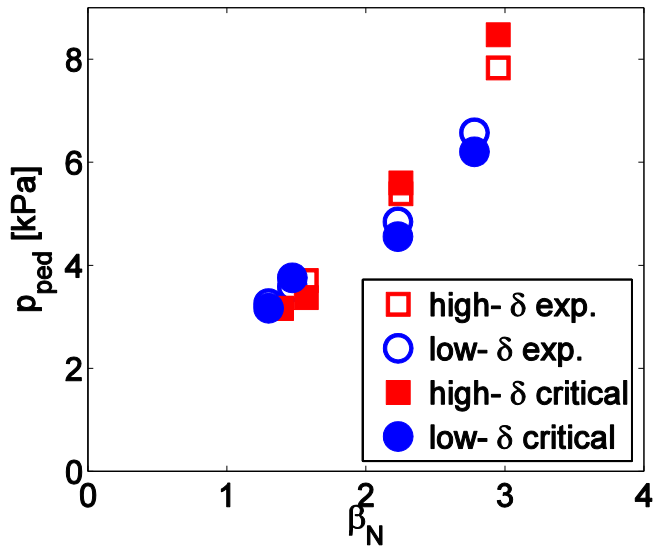


Figure 2. The measured and self-consistently modelled pedestal heights as a function of global  $\beta_N$ .

It should be noted that the stability improvement with increasing core pressure is only seen with low gas injection rates. When the gas injection is increased, the beneficial effect of the core pressure is strongly reduced [18]. It is not entirely clear why the pedestal improvement by high core pressure is lost at high gas rates, but it would be consistent with the stability picture at low pedestal current density at which part of the stability diagram the improvement due to increased  $\beta_N$  is reduced.

#### IV. NITROGEN SEEDING

In JET with Be/W wall (ITER-like-wall or JET-ILW) high triangularity baseline plasmas ( $\beta_N < 1.5$ ) operating at high gas fuelling to avoid tungsten influx, the confinement has been degraded by 40% compared with earlier experiments with carbon wall (JET-C) with same heating power and density [19]. The lower confinement is mainly due to lower pedestal temperature [20]. However with nitrogen seeding the pedestal and the global confinement can be partially recovered. The confinement improvement with nitrogen seeding is more modest in low triangularity [20]. In JET-C the dominant impurity in the edge region was carbon, leading to  $Z_{\text{eff}} \approx 2.0$ , whereas in JET-ILW

without impurity seeding the main impurity is beryllium, leading to  $Z_{\text{eff}} \approx 1.2$  [19]. In nitrogen seeded discharges nitrogen becomes the main impurity and  $Z_{\text{eff}}$  increases to similar level as in JET-C [19]. The uncertainty in the  $Z_{\text{eff}}$  measurements is about 20%.

One of the major differences between JET-ILW without seeding and JET-C plasmas is the lower radiation in the divertor region due to the lack of low-Z impurities such as carbon [19]. Nitrogen seeding allows return to high divertor radiation. Simulating the effect of nitrogen seeding using the EDGE2D-Eirene code of the steady-state inter-ELM H-mode plasma, including the sputtered beryllium as an intrinsic impurity is able to reconstruct good agreement in radiation power in the divertor region with nitrogen seeding [21]. EDGE2D-Eirene is also able to reconstruct the electron temperature at the outer midplane separatrix (where the high resolution Thomson scattering system is located) as a function of nitrogen content in the computational domain (Fig. 3). In this simulation  $I_p$ ,  $B_t$  and the power arriving at the pedestal top are the same as in experiment and the diffusivities are kept fixed assuming no change in pedestal transport with the nitrogen seeding. The separatrix temperature falls 30 eV as the amount of nitrogen is increased. The initial drop (from zero to finite amount of nitrogen) might be exaggerated, since no other impurities but beryllium were assumed to be present. In order to be conservative, we assume a 20 eV drop in  $T_{e,\text{sep}}$  as a result of seeding nitrogen in the following analysis. The purpose of the following stability analysis is to explore the qualitative trends that the drop in separatrix temperature and the consequent shift of the profiles have on the marginal peeling-ballooning mode stability of the pedestal, not to reproduce the observed pedestal increase exactly.

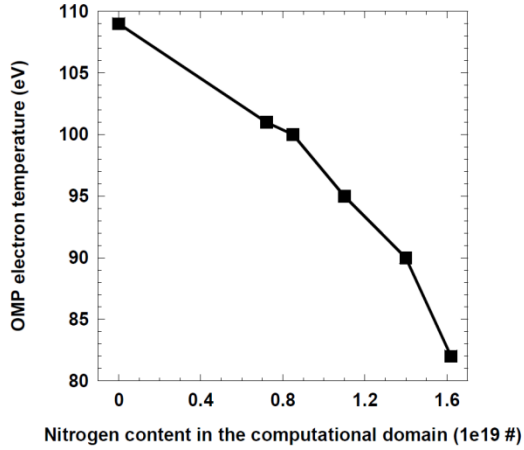


Figure 3. EDGE2D-EIRENE predicted electron temperature at the outer midplane separatrix as a function of nitrogen content in the computational domain (number of atoms).

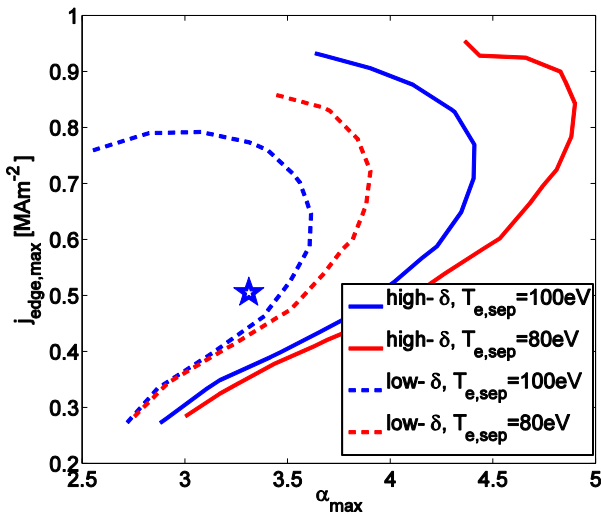


Figure 4. The effect of the assumed separatrix temperature on stability boundaries for low (dashed) and high (solid) triangularities

To test the effect of  $T_{e,sep}$  on the stability we use an unseeded JET discharge #82806, ( $B_t=2.7T$ ,  $I_p=2.5MA$ ,  $\beta_N=1.1$ ). We vary the separatrix temperature and shift the profiles accordingly. The effect on the low ( $\delta=0.2$ ) and high ( $\delta=0.4$ ) triangularity stability boundaries is shown in Figure 4. The main difference in the stability boundaries is in the high- $\alpha$  part at high current where the intermediate-n peeling-ballooning modes are the limiting instability, while the low current part with high-n

ballooning modes is hardly changed by the shift of the profiles. The small improvement in the ballooning stability agrees with the local  $n=\infty$  ballooning mode stability, which does not change at all with the shift. It should also be noted that the stability improvement is larger for the high triangularity case. In a self-consistent analysis we find an increase of 10% in critical temperature pedestal height for a decrease of 10% in  $T_{e,sep}$ .

We also vary the charge number of the impurity ( $Z_{imp}$ ) with fixed  $Z_{eff}$  and  $T_{e,sep}$  in the simulation to determine the effect different impurities have on the pedestal stability.  $Z_{imp}$  enters the equilibrium reconstruction in two ways: Low  $Z_{imp}$  leads to more ion dilution and, thus, lower pressure gradient; and impurities with low  $Z_{imp}$  also reduce the bootstrap current more than high  $Z_{imp}$  impurities for a given value of  $Z_{eff}$ . When these effects are combined in a self-consistent simulation, we see a monotonic decrease of marginally stable  $T_{e,ped}$  as a function of  $Z_{imp}$  of about 5% between beryllium ( $Z_{imp}=4$ ) and neon ( $Z_{imp}=10$ ). Since the marginally stable  $T_{e,ped}$  decreases with  $Z_{imp}$ , the seeding with high-Z impurities is unlikely to be beneficial unless it can reduce  $T_{e,sep}$  further. The high-Z impurities also radiate more strongly in the pedestal and the core than nitrogen, which is also detrimental to reaching high  $T_{e,ped}$ .

We combine all the effects and take into account expected pedestal widening as the height increases with the relation:  $\Delta \sim \sqrt{\beta_{p,ped}}$  ( $\Delta$  is the width of the pedestal and  $\beta_{p,ped}$  is the poloidal  $\beta$  at the top of the pedestal). This relation is used in a predictive EPED1 model [22] and seen to be valid in JET-C (although not distinguishable from constant real space width combined with flux compression) [23] and in JET-ILW with nitrogen seeding [24]. Figure 5 shows the result of the self-consistent analysis at fixed  $Z_{eff}=1.5$  for beryllium and nitrogen impurities for two separatrix temperatures, 80 and 100eV. Beryllium as an impurity reaches higher pedestal for both assumed values of  $T_{e,sep}$ . However, as was shown in Figure 3, it is the nitrogen seeding that leads to lower  $T_{e,sep}$ . Therefore, the comparable modelled values are nitrogen at  $T_{e,sep}=80$ eV and beryllium at  $T_{e,sep}=100$  eV. We can



for the very favourable power scaling found in JET [17]. The possibility of affecting the pedestal stability (and, through that, plasma confinement) with impurities opens new possibilities for future devices that are in any case going to have to radiate a large fraction of the fusion power using extrinsic impurity seeding. However, more modelling and experiments are needed to fully understand the effects the impurities have on the pedestal and to optimise the right impurity seeding for each device.

#### **ACKNOWLEDGEMENTS**

This work has been carried out within the framework of the EUROfusion Consortium and has received funding from the European Union's Horizon 2020 research and innovation programme under grant agreement number 633053 and from the RCUK Energy Programme [grant number EP/I501045]. To obtain further information on the data and models underlying this paper please contact [PublicationsManager@ccfe.ac.uk](mailto:PublicationsManager@ccfe.ac.uk). The views and opinions expressed herein do not necessarily reflect those of the European Commission.

#### **REFERENCES**

- [1] F. Ryter, C. Angioni, M. Beurskens, S. Cirant, G.T. Hoang, G.M.D. Hogeweij, F. Imbeaux, A. Jacchia, P. Mantica, W. Suttrop and G. Tardini, *Plasma Phys. Control. Fusion* **43** (2001) A323.
- [2] J.E. Kinsey G.M. Staebler, J. Candy, R.E. Waltz and R.V. Budny., *Nucl. Fusion* **51** (2011) 083001.
- [3] S. Saarelma A. Alfier, M.N.A. Beurskens, R. Coelho, H.R. Koslowski, Y. Liang, I. Nunes and JET EFDA contributors, *Plasma Phys. Control. Fusion* **51** (2009) 035001.
- [4] P.B. Snyder, H.R. Wilson, J.R. Ferron, L.L. Lao, A.W. Leonard, D. Mossessian, M. Murakami, T.H. Osborne, A.D. Turnbull and X.Q. Xu. *Nucl. Fusion* **44** (2004) 320.
- [5] G. Saibene , N. Oyama, J. Lönnroth, Y. Andrew, E. de la Luna, C. Giroud, G.T.A. Huysmans, Y. Kamada, M.A.H. Kempenaars et al., *Nucl. Fusion* **47** (2007) 969.
- [6] P.B. Snyder, N. Aiba, M. Beurskens, R.J. Groebner, L.D. Horton, A.E. Hubbard, J.W. Hughes, G.T.A. Huysmans, Y. Kamada, A. Kirk et al., *Nucl. Fusion* **49** (2009) 085035.
- [7] R. Pasqualotto, P. Nielsen, C. Gowers, M. Beurskens, M. Kempenaars, T. Carlstrom, D. Johnson and JET-EFDA Contributors, *Rev. Sci. Instrum.* **75**, (2004) 3891.

- [8] L. Frassinetti L M. N. A. Beurskens, R. Scannell, T. H. Osborne, J. Flanagan, M. Kempenaars, M. Maslov, R. Pasqualotto, M. Walsh and JET-EFDA Contributors., *Review of Sci. Instr.*, **83** (2012) 013506.
- [9] R. Scannell, M. J. Walsh, P. G. Carolan, A. C. Darke, M. R. Dunstan, R. B. Huxford, G. McArdle, D. Morgan, G. Naylor, T. O’Gorman, S. Shibaev, N. Barratt, K. J. Gibson, G. J. Tallents and H. R. Wilson, *Rev. Sci. Instrum.* **79** (2008) 10E730.
- [10] R.J. Groebner M.A. Mahdavi, A.W. Leonard, T.H. Osborne and G.D. Porter., *Plasma Phys. Contr. Fusion*, **44**, (2002) A265.
- [11] A. Kallenbach , N. Asakura, A. Kirk, A. Korotkov, M.A. Mahdavi, D. Mossessian, G.D. Porter, *J. of Nucl. Mater.* **337-339** (2005) 381.
- [12] R Simonini, G. Corrigan, G. Radford, J. Spence and A. Taroni, *Contributions to Plasma Physics* **34**, (1994), 368 – 373.
- [13]. D. Reiter, *Journal of Nuclear Materials* **196 – 198**, (1992), 80 – 89.
- [14]. S. Wiesen, EDGE2D/EIRENE code interface report, JET ITC-Report, [http://www.eirene.de/e2deir\\_report\\_30jun06.pdf](http://www.eirene.de/e2deir_report_30jun06.pdf), 2006.
- [15] O. Sauter, C. Angioni and Y. R. Lin-Liu, *Phys. Plasmas* **6** (1999) 2834.
- [16]H.R. Wilson, P.B. Snyder, G.T.A. Huysmans, R.L. Miller, *Phys. Plasmas* **9** (2002) 1277.
- [17] C. Challis J. Garcia, M. Beurskens, P. Buratti, P. Drewelow, L. Frassinetti, C. Giroud, N. Hawkes, J. Hobirk, E. Joffrin et al. *Proceedings of the 25<sup>th</sup> IAEA FEC, 13-18 Oct. 2014, Saint Petersburg, Russia.* EX/9-3
- [18] C.F. Maggi, S. Saarelma, M. Beurskens, C. Challis, I. Chapman, E. de la Luna, J. Flanagan, L. Frassinetti, C. Giroud, J. Hobirk et al. *Proceedings of the 25<sup>th</sup> IAEA FEC, 13-18 Oct. 2014, Saint Petersburg, Russia.* EX/3-3
- [19] C. Giroud, G.P. Maddison, S. Jachmich, F. Rimini, M.N.A. Beurskens, I. Balboa, S. Brezinsek, R. Coelho, J.W. Coenen, L. Frassinetti, E. Joffrin et al. *Nucl. Fusion* **53** (2013) 113025.
- [20] C. Giroud , S.Jachmich, P. Jacquet, A. Jarvinen, E. Lerche, F. Rimini, L. Aho-Mantila, N. Aiba, I. Balboa et al. *submitted to Plasma Phys. Contr. Fusion* (2014).
- [21] A. Järvinen , M. Groth, M. Airila, P. Belo, M. Beurskens, S. Brezinsek, M. Clever, G. Corrigan, S. Devaux, P. Drewelow et al. , *Proc. of 21th Conf. on Plasma Surface Interactions, 26-30 May, 2014, Kanazawa, Japan.*
- [22] P. B. Snyder, R. J. Groebner, A. W. Leonard, T. H. Osborne, and H. R. Wilson, *Phys Plasmas* **16**, (2009) 056118.
- [23] M. N. A. Beurskens, T. H. Osborne, P. A. Schneider, E. Wolfrum, L. Frassinetti, R. Groebner, P. Lomas, I. Nunes, S. Saarelma, R. Scannell et al. *Phys. Plasmas* **18** (2013) 056120

[24] M.J. Leyland, M.N.A. Beurskens, L. Frassinetti, C. Giroud, S. Saarelma, P.B. Snyder, J. Flanagan, S. Jachmich, M. Kempenaars, P. Lomas et al. "The H-Mode Pedestal Structure and its Role on Confinement in JET with a Carbon and Metal Wall", accepted for publication in Nucl. Fusion

[25] M.N.A. Beurskens, L. Frassinetti, C. Challis, T. Osborne, P.B. Snyder, B. Alper<sup>1</sup>, C. Angioni, C. Bourdelle, P. Buratti, F. Crisanti et al. Nucl. Fusion **53** (2013) 013001.